Functional Materials 15, No.4 (2008)

On the cellular structure period of the crystallization front of a binary melt

V.N.Kanischev, S.V.Barannik*

Institute for Single Crystals, STC "Institute for Single Crystals", National Academy of Sciences of Ukraine, 60 Lenin Ave., 61001 Kharkiv, Ukraine
*Institute for Scintillation Materials, STC "Institute for Single Crystals", National Academy of Sciences of Ukraine, 60 Lenin Ave., 61001 Kharkiv, Ukraine

Received May 21, 2008

The impurity diffusion problem in a melt being crystallized at small distortions of the phase interface has been solved within a bidimensional model for steady-state mode. The cellule width so calculated has been shown to correspond to the crystallization rates several times lower than those obtained by other authors in experiment. The cellular structure of the phase interface observed by those authors after the melt was decanted is supposed to be formed during a transition process consisting of two steps. In the first one, a periodic structure with insignificant bulges was formed. In the second step, the bulge height but not width was changed right to the crystallization process was attained the steady state.

В двумерной модели в установившемся режиме решена задача по диффузии примеси в расплаве, который кристаллизуется при малых искривлениях границы раздела фаз. Показано, что рассчитанная при этом ширина ячеек соответствует скоростям кристаллизации, которые в несколько раз меньше, чем полученные в эксперименте другими авторами. Высказано предположение, что наблюдаемая этими авторами после декантации расплава ячеистая структура поверхности раздела образовалась во время переходного процесса, состоящего из двух этапов. На первом из них возникла периодическая структура с небольшими выступами. На втором этапе, вплоть до выхода процесса кристаллизации на стационарный режим, изменялась высота выступов, но не их ширина.

The periodicity is a remarkable cellular structure property of a binary melt crystallization front arising under certain conditions. The crystals grown in such conditions (Fig. 1a [1]) find not any applications in the meantime, in contrast to, e.g., similar nanostructured materials (Fig. 1b [2]), it is of some interest to study the nature of cell formation at the crystallization front. In fact, the formation of any periodical structure is based on a self-organization process in a non-equilibrium system, and the knowledge obtained for one of such systems will be no doubt useful in obtaining other periodic structures.

In [3, 4], the transition from a flat phase interface to its periodical defect structure was studied using the variation method. The criterion we have obtained for such a transition agrees with conditions determined by another technique [5]. Nevertheless, we have not considered to date the agreement of the calculated cellular structure period values with literature data on the cell width. This work is intended to fill that gap.

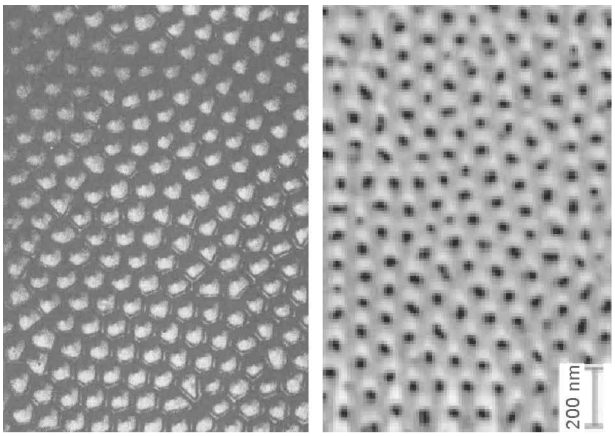

Fig. 1. a) Phase interface structure after decantation of Pb + 0.15% Sn melt [1]. The average bulge spacing in 58.8 μm. b) Plan view of mesoporous aluminum oxide film [2]

We shall use in this study mainly the results by Tiller and Rutter [1] who have collected a comprehensive experimental data set on formation of various phase interface morphologies at crystallization of lead with tin admixture. In particular, according to those data, the width of linearly elongated cells exceeds the hexagonal cell dimensions by 20 to 30% only. Therefore, the conclusions drawn within the frame of bidimensional solidification model can be expected to be applicable to the tridimensional case.

Let the bidimensional solidification model for a binary melt be considered where the temperature field is specified as a linear function of the coordinate x directed towards the crystallization front movement at a constant speed V [6]. Let the impurity concentration in the melt $C(x,y)$ be laid off in $C_0(1–k)/k$ units from the C_0 level where C_0 is the impurity concentration in the melt at infinite distance from the crystallization front (CF) and k, the impurity distribution coefficient. The coordinate x will be laid off in L units where L is the cell half-width or the half-period of CF line defined by equation $x=\varphi(y)$.

Let the following dimensionless coefficients be introduced:

$$\kappa = \frac{D}{VL}, \tag{1}$$

$$B = \frac{kGD}{(k-1)mVC_0}, \tag{2}$$

$$\gamma = \frac{kT_mV\Gamma}{(k-1)mDC_0}, \tag{3}$$

where G is the temperature gradient, K/cm; m, the liquidus line slope in the phase diagram of the binary system, K/%; Tm, the solidification point of the pure melt; Γ, the capillary constant, cm.

Then the problem of the impurity bidimensional diffusion in the melt being crystallized at a constant rate can be formulated as

$$C_{xx} + C_x + \kappa^2 C_{yy} = 0, \tag{4}$$

$$C_x(\varphi(y)) - \kappa^2\varphi_y(y)C_y(\varphi(y)) + (1 - k)C(\varphi(y)) + k = 0, \tag{5}$$

$$C(\varphi(y)) = 1 - B\varphi(y) + \gamma\kappa^2\varphi_{yy}(1 + \kappa^2\varphi_y^2)^{-3/2} = 0, \tag{6}$$

$$C(\infty, y) = 0,\ C_y(x,0) = C_y(x,1) = 0. \tag{7}$$

Here, the indices is used to denote partial derivatives of $C(x,y)$ with respect to x and y as well as that of $\varphi(y)$ with respect to y. Eq. (5) is the condition of impurity conservation at the CF. Eq. (6) relates the impurity concentration at the phase interface to thermodynamic characteristics of the latter. It follows from the phase diagram and the Gibbs-Thomson condition. The second and third conditions from (7) reflects the experimental fact that the cell is symmetrical with respect to its middle.

When being restricted to small amplitudes ξ of the cell bulges, the solution of the problem in the second approximation with respect to ξ can be presented [3] as

$$C(x,y) = e^{-x} + A_1\xi\exp(-q_1x)\cos\pi y + \xi^2[A_0e^{-x} + A_2\exp(-q_2x)\cos 2\pi y], \tag{8}$$

$$\varphi(y) = \xi\cos\pi y + \xi^2(\alpha_0 + \alpha_2\cos 2\pi y), \tag{9}$$

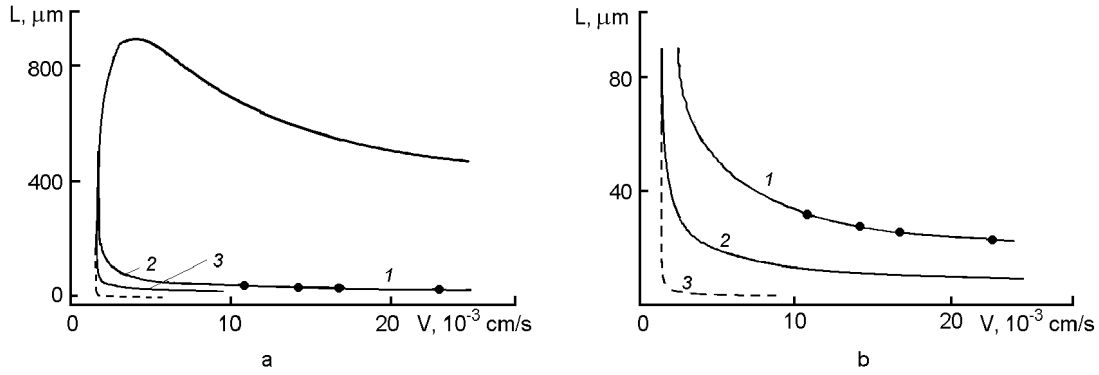

Fig. 2. (a) Dependence of the phase interface half-period L on the crystallization speed V at different values of capillary constant Γ (cm): $\Gamma=7.43\cdot10^{-8}$ (1), $\Gamma=1\cdot10^{-8}$ (2), $\Gamma=10^{-10}$ (3). The separated points are experimental ones taken from [1]; (b) the image (a) in enlarged vertical scale.

where

$$q_n = 0.5 + \sqrt{0.25 + (n\pi\kappa)^2}\,. \tag{10}$$

Let the solutions (8), (9) be substituted into each of (5), (6), the exponents be expanded into Taylor series, the items with common factors $\xi\cos\pi y$, ξ^2, $\xi^2\cos2\pi y$ be grouped together and the sums thereof be set to zero. Thus, a system of six equations is obtained from which we get

$$B + \pi^2\kappa^2\gamma = \frac{q_1 - 1}{q_1 + k - 1}, \tag{11}$$

$$A_1 = 1 - B - \pi^2\kappa^2\gamma,\ A_0 = \frac{1}{2}\left(A_1 q_1 - \frac{1}{2}\right),$$

$$A_2 = \frac{kA_0(A_\gamma - 1)}{A_\gamma(q_2 + k - 1) - k},\ \alpha_0 = 0,\ \alpha_2 = A_2\frac{q_2 + k - 1}{k} - A_0, \tag{12}$$

where $A_\gamma = 1 - B - 4\pi^2\kappa^2\gamma$.

It is easy to transform the Eq. (10) at n = 1 into the equality

$$\pi^2\kappa^2 = q_1(q_1 - 1). \tag{13}$$

Substituting (13) into (11), we get a cubic equation

$$\gamma q_1^3 + \gamma(k-2)q_1^2 + [B - \gamma(k-1) - 1]q_1 + B(k-1) + 1 = 0, \tag{14}$$

the solution thereof, $q_1 = q_s(k, B, \gamma)$, depends on the input parameters of the problem (4)-(7). Substituting that solution into (13) ant taking into account (1), we get the dependence of the defect structure half-period at the interphase surface, L, on the crystallization speed, V, in the form

$$L = \frac{\pi D}{V\sqrt{q_s(q_s - 1)}}. \tag{15}$$

Note that the crystallization speed enters the right-hand part of Eq. (16) also via the dependence $q_s(B(V), \gamma(V))$.

Besides the function $L(V)$ itself having the typical positive branches shown in Fig. 2, we shall need further the abscissa of its boundary point V_b. That point is characteristic in that at $V<V_b$, the solution of the problem (4)-(7) can be only flat one. Each branch of $L(V)$ has its corresponding root of

Eq. (14). In the boundary point, both roots are equal to one another and thus, the derivative of the left-hand part of (14) with respect to q_1 is zero:

$$3\gamma q_1^2 + 2\gamma(k-2)q_1 + B - \gamma(k-1) - 1 = 0. \tag{16}$$

It is just the system of equations (14), (16) where V_b is determined from.

The parameter γ for metals has been estimated to be small. For example, it amounts $3.7\cdot10^{-4}$ for the curve 2 of Fig. 2. Then, eliminating the parameter q_1 between Eqs. (14), (16) and rejecting in the equation obtained the items with γ in a power exceeding 1, it is easy to get the formula

$$B_b = 1 - 3\sqrt[3]{k^2\gamma_b/4}, \tag{17}$$

where the parameters B and γ are determined at the boundary value $V=V_b$. At a further consideration of Eq. (17) as an implicit dependence of V_b on $\Gamma^{1/3}$, at first approximation with respect to $\Gamma^{1/3}$ we get

$$V_b = V_0\left\{1 + 3k\left[\frac{T_m V_0 \Gamma}{4(k-1)mDC_0}\right]^{1/3}\right\}, \tag{18}$$

where

$$V_0 = \frac{kGD}{(k-1)mC_0} \tag{19}$$

is the critical crystallization speed in the classic solidification theory determined from the condition of crystallization overcooling (C.O.) of the melt [7].

The formulas (17) and (18) in another notation are presented in [6], [8], respectively, where those have been obtained using the linear analysis of the flat crystallization front disturbances. Thus, according to (18), the transition to non-planar phase interface must occur at higher critical crystallization speeds (V_c) than those predicted by the C.O. criterion. Nevertheless, numerous experiments, including the data from [1], have shown an agreement with the formula [19] but not with (18). The problem of that discrepancy requires a special consideration and falls outside the limits of this study. It is to note only that there is nothing that might hinder us to use the relationship $C_0 \sim G/V_c$ as an experimental fact.

Let the calculation results to be considered with the data by Tiller and Rutter [1] on the Pb+0.15% Sn alloy when studying the dependence of hexagonal cell width a on the crystallization speed V. In Table 1, the results from this study are presented by four sets of values (G_a, V_a, L_a), where $L_a \equiv a/2$.

Fig. 2 shows the $L(V)$ dependence plots calculated using (15) for the case G = 7 K/cm. It will be seen from what follows that only lower branches of the $L(V)$ plots are of a practical interest, that is why those are presented in Fig. 2b at an extended vertical scale. The following parameters were used when constructing the plots of Fig. 2: k=0.56, T_m=600 K, C_0=0.15%, μ= -3 K/%, $D=7\cdot10^{-5}$ cm^2/s [1]. The only undetermined quantity was the surface tension coefficient Γ that was assumed to have the values corresponding to three cases. In the first one (curve 1), the $\Gamma=\Gamma_a$ value was selected so that the calculated curve passed the experimental point with coordinates given in the last row of Table 1. The so calculated Γ_a values as well as the corresponding boundary crystallization speed values V_b for all the four (G_a, V_a, L_a) sets are presented in Table 1. In the second case (curve 2), the $\Gamma=1\cdot10^{-8}$ cm was used that is assumed usually in theoretical studies of the phase interface morphology [5, 9]. In Table 1, the boundary crystallization speed values V_{b1} are presented for that case. Finally, when constructing the curve 3, a negligible value 10^{-10} cm was ascribed to the parameter Γ.

In Fig. 2, experimental points are shown as well with ordinates normalized to the unique temperature gradient G=7 K/cm. The small deviations thereof from the curve 1 of Fig. 2b are due to the scatter in Γ_a values.

Table 1: Dependence of capillary constant Γ_a and the boundary crystallization speed V_b on the temperature gradient G_a, crystallization speed V_a, and the cell half-width L_a calculated from experimental data [1].

G_a, K/cm	V_a, 10^{-3} cm/s	L_a, mkm	Γ_a, 10^{-8} cm	V_b, 10^{-3} cm/s
4.15	10.8	29.4	6.72	0. 964
4.65	14.2	25.4	6.60	1.09
4.85	16.7	24.2	7.02	1.14
7.0	23.0	21.6	7.43	1.7

Prior to consideration of the data presented in Fig. 2, the following features of the $L(V)$ plot are worth to be noted. The upper branches of $L(V)$ at different Γ values, other conditions being the same, are essentially merged together starting from speeds somevhat exceeding V_b. In contrast, the lower $L(V)$ branch approaches to the line L = 0 (curve 3 of Fig. 2b) as Γ decreases and turns thereto at $\Gamma = 0$.

It is seen from Fig. 2 that it is just the lower $L(V)$ branch that corresponds to the experimental values of the cell width that are typical of metal systems [1]. Indeed, in the upper branches of plots in Fig. 2a the value V=0.023 cm/s corresponds to the cell half-width of $L\approx$490 μm exceeding the experimental value by a factor more than 20. Taking this fact into account, the model with a negligible surface tension at the phase interface can be discarded at once, since the cell size obtained within its frame will be either too large (upper branch) or near to zero (lower branch). It is to note here that the cell size of about 10 μm in metals is explained just by the fact that $\Gamma\approx10^{-8}$ cm in this case [7]. It is of interest that if the capillary constant might be reduced down to $1.84\cdot10^{-12}$ cm, the plot of Fig. 2 would pass the point with coordinates V=0.023 cm/s and L=100 nm (a typical size of nanostructures [2]).

The rather high Γ_a values (see Table 1) as compared to the value $\Gamma=1\cdot10^{-8}$ cm typical of metals are worth to attention. At the same time, the curve 2 corresponding to that value (Fig. 2) is positioned considerably below the experimental popints. However, a detailed consideration of the capillary constant choice testifies to the value $\Gamma=1\cdot10^{-8}$ cm.

First of all, let the boundary speed values V_b (Table 1) and V_{b1} (Table 2) be compared with the critical crystallization speed V_c. For the Pb + 0.15% Sn alloy, the pox-like phase interface was revealed at G=13 K/cm and $V=V_c=2.84\cdot10^{-3}$ cm/s [1]. To determine the V_c for each $G=G_a$, let the relationship $C_0 \sim G/V_c$ be used (see above). It is seen from Tables 1 and 2 that the boundary speed values V_{b1} calculated for $\Gamma=1\cdot10^{-8}$ cm are much more similar to the critical speeds V_c than V_b ones calculated for $\Gamma\approx7\cdot10^{-8}$ cm.

In addition to the above, it is to note that the transition to a regular cellular structure was observed in [1] at crystallization speeds near about $2V_c$. It is seen from Tables 1 and 2 that the half-period values L_r in the cellular structure calculated at $\Gamma=1\cdot10^{-8}$ cm and $V=2V_c$ exceed only slightly the experimental L_a values. This testifies also to the value $\Gamma=1\cdot10^{-8}$ cm.

Finally, it is to take into account that the cell dimensions in [1] were measured for samples

Table 2: Dependence of boundary crystallization speed V_{b1}, critical crystallization speed V_c, and the regular cellular structure half-period L_a on the temperature gradient G_a calculated for the capillary constant $\Gamma=1\cdot10^{-8}$ cm.

G_a, K/cm	V_{b1}, 10^{-3} cm/s	V_c, 10^{-3} cm/s	L_r, mkm	V_a / V_c
4.15	0.890	0. 907	35.5	11.9
4.65	1.00	1.02	33.5	13.9
4.85	1.05	1.06	32.6	15.8
7.0	1.53	1.53	27.0	15.0

grown at speeds exceeding the critical ones by a factor of 12-16 (see Table 2). The use of such crystallization speeds exceeding considerably not only the critical one but also the speed at which the cellular structure becomes a regular one is explained most likely by the authors' effort to obtain a well-defined cellular pattern that requires a rather high cell bulges. In that case, however, our calculations at $\Gamma \approx 7 \cdot 10^{-8}$ cm cannot be considered as correct ones, since the call bulge amplitude was assumed to be small at all the crystallization speeds, including $V=V_a$.

Taking the above into account, it is natural to make an assumption that will be formulated after the remark that follows. It is known [10] that the approach of a binary melt crystallization process to the stationary mode at the growth renewing (or after its onset) is preceded by a transient period that continues until the stationary distribution of temperature and impurity is attained in the crystal and melt in a mobile system of coordinates. It follows therefrom that the crystallization speed V may differ considerably from the crystal pulling speed W, especially shortly after the pulling device is switched on (or after the electrical scheme is switched on for the temperature field displacement as in [1]).

The assumption mentioned consists in that the cellular structure used in [1] to measure the cell size was formed during at least two stages of the transient crystallization period. The first initial stage occurred at the speed increasing from zero to $2V_c$ and finished by formation of a regular structure with small bulges at the phase interface. At the second stage, the bulge spacing remained unchanged but the bulge height increased till the crystallization speed had attained the temperature field displacement speed W. This assumption is confirmed by the known fact of the cellular structure stability. For example, it has been found for a Pb+Sb alloy [11] that the cell width arising at a certain crystallization speed V_1 remains unchanged at the subsequent speed increase up to $V_2=2V_1$.

Thus, when a certain boundary crystallization speed $V=V_b$ is exceeded, the problem (9)-(12) has a non-planar solution ($\xi \neq 0$). However, this does not mean at all that the crystallization front will take a cellular structure at $V>V_b$. This can occur only if the cellular surface of the phase interface is more stable than the flat one. In the stationary problem corresponding to the steady state crystallization mode, the conditions of transition to the cellular growth can be determined by comparing the dissipation energy prior to and after such a transition. The temperature field being preset in that case, only the diffusion component of the dissipation energy will change at the transition from the flat boundary to the curved one. The latter can be associated [12] with the functional

$$I\{C(x,y),\varphi(y)\} = \int_0^1 dy \int_{\varphi}^{\infty} e^x \left(C_x^{\,2} + \varepsilon^2 C_y^{\,2}\right) dx - \int_{(\varphi\}} e^x [2k + (1-k)C]C dy\,, \qquad (20)$$

where (φ) means the line $\varphi=x(y)$ along which the line contour integral is taken. In fact, the first integral in (20) is in proportion to the energy being dissipated as the impurity diffuses in the melt volume [4]. This is evidenced, in particular, by the dependence of its integrand on the squared concentration gradient. The second part can be presented as

$$\frac{k^2}{1-k} \int_{(\varphi)} e^x dy - \frac{1}{1-k} \int_{(\varphi)} e^x \left[C_x - \varepsilon^2 \varphi_y C_y\right]^2 dy\,. \qquad (21)$$

using the boundary condition (5). It is seen that at the fixed phase interface, the curvilinear part of the functional (20) consists of an item inessential at variation and an integral with integrand being in proportion to the squared concentration gradient but related to the phase interface. Thus, by analogy with double integral, the curvilinear integral in (20) can be considered to be in correspondence to the energy being dissipated at the phase interface as the impurity particles pass from the liquid phase to the solid one.

In fact, when having determined the boundary shape by Eq. (9), we go from the problem (4)-(7) to its variational equivalent. Having calculated the second variation of the functional (20), it is easy to establish that, at least in the case $k>1$, the solution of the problem (4)-(7) gived to the functional

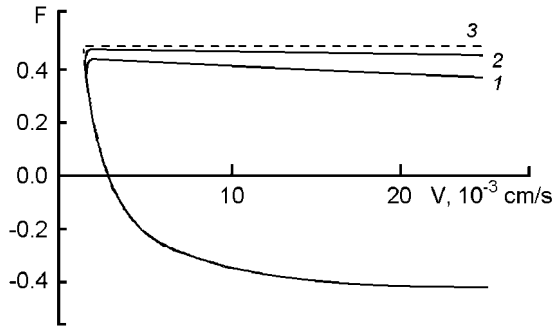

Fig. 3. Dependence of F factor on on the crystallization speed V at different values of capillary constant Γ (cm): $\Gamma=7.43\cdot10^{-8}$ (1), $\Gamma=1\cdot10^{-8}$ (2), $\Gamma=10^{-10}$ (3).

(20) not simply stationary value but the minimum one. However, there are grounds to suppose [12] that the stationary value of the functional (20) is equivalent to its minimum one within the whole range of k values.

Substituting (8), (9) into (20) and taking into account (11), (12), we get at an accuracy to ξ^2:

$$I = -k + \xi^2 \frac{k}{2} F \,, \tag{22}$$

where

$$F = B + \pi^2 \kappa^2 \gamma - \frac{1}{2} \,. \tag{23}$$

It is seen from (22) that the functional (20) value at the phase interface distortion in the form of a periodic function ($\xi\neq0$) will be smaller than the value corresponding to the planar case ($\xi=0$) if the factor F will be negative. It is to note that the dissipation energy for defects distributed chaotically over the surface may differ from that for salf-organized periodic structure. We cannot say nothing about the energy in the first case, since the solution of the problem was supposed to be periodic at its formulation.

Fig. 3 shows the $F(V)$ plots constructed for the same parameter values as for the curves in Fig. 2. Comparing the Figs. 2 and 3, it is easy to understand that the upper branches of the curves in Fig. 2 correspond to the lower branches of Fig. 3 ones and vice versa. First, both upper $L(V)$ branches and lower $F(V)$ ones merge together as the crystallization speed increases. Second, the almost horizontal lower branch of curve 3 in Fig. 2 corresponds to the almost horizontal upper branch of curve 3 in Fig. 3.

It has been shown above that it is just the lower branches of $L(V)$ plots that correspond to the experiment [1]. The upper branches of corresponding $F(V)$ curves cannot be supposed to intersect the $F=0$ line at any reasonablr crystallization speed. Thus, there is a contradiction associated most likely with imperfection of our solidification model. This problem of great interest will be considered in detail in a next work.

To conclude, in spite of a considerable amount of available experimental data on the problem of binary melt solidification, it is obviously insufficient to check the validity of the corresponding theory.

References

1. W.A.Tiller, J.W.Rutter, *Can. J. Phys.* **34**, 96 (1956).
2. The Red Book of Microstructures of Novel Functional Materials, ed. D. Tretyakov, Moscow, MGU, (2006) [in Russian].
3. V.N.Kanischev, *Kriystallografiya,* **49**, 1151, (2004).
4. V. N. Kanischev, S. V. Barannik, *Kristallografiya* **51**, 124 (2006).
5. W. W. Mullins, R. F. Sekerka, *J. Appl. Phys.* **35**, 444 (1964).
6. J. S. Langer, *Rev. Mod. Phys.* **52**, 1 (1980).

7. W. A. Tiller. Crystal Growth from a Melt, in: The Art and Science of Growing Crystals, John Wiley & Sons, Inc., New York – London (1963).
8. R. F. Sekerka, *J. Appl. Phys.* **36**, 264 (1965).
9. D. J. Wollkind, R. Sriranganathan, D. B. Oulton, *Physica D* **12**, 215 (1984).
10. S. V. Barannik, A. Ya. Dan'ko, V .N. Kanischev, *Functional Materials,* **4**, 551 (1997).
11. L. R. Morris, W. C. Winegard, *J. Crystal Growth,* **5**, 361 (1969).
12. V. N. Kanischev, S. V. Barannik, *Functional Materials,* **13**, 558 (2006).

Про період комірчастої структури фронту кристалізації бінарного розплаву

В.Н.Каніщев, С.В.Баранник

У двовимірній моделі в усталеному режимі розв'язано задачу дифузії домішки у розплаві, що кристалізується при незначних викривленнях межі розділу фаз. Показано, що при цьому ширина комірок відповідає швидкостям кристалізації, у кілька разів меншим від одержаних в експерименті іншими авторами. Висловлено припущення, що комірчаста структура поверхні розділу, яка спостерігалася цими авторами після декантації розплаву, утворилася під час перехідного процесу, що складається з двох етапів. На першому етапі виникла періодична структура з невеликими виступами. На другому етапі, аж до виходу процесу кристалізації на стаціонарний режим, змінювалася висота виступів, але не їхня ширина.